Int. J. Nano Dimens., 13 (4): 362-373, Autumn 2022

ORIGINAL ARTICLE

# Synthesis and characterization of bioglass / maltodextrin nanocomposites in the presence of PVP as a potential candidate for flutamide drug delivery

*Masoumeh Tajik*[1], *Mirabdullah Seyed Sadjadi*[1,*], *Karim Zare*[1], *Nazanin Farhadyar*[2]

[1]*Department of Chemistry, Science and Research Branch, Islamic Azad University, Tehran, Iran*
[2]*Department of Chemistry, Varamin Pishva Branch, Islamic Azad University, Varamin, Iran*

Received 24 May 2022; revised 30 June 2022; accepted 12 July 2022; available online 18 July 2022

**Abstract**

Bioactive glass is an appropriate substance for the transporting a pharmaceutical compound owing to its special effects (containing great antibacterial, semiconducting, nanoporous, adherent, and strong bonding with the bone tissue). Hence, in recent years, many investigations have been done in this topic. However, several constraints alike fast drug release and slow drug loading ability are observed in preceding researches. The researchers proposed that restrictions can be resolved by improving the fabricating method of bioglass and the reinforcement of diverse nanocomposites for postponing drug release. Therefore, new bioglass/maltdextrin nanocomposites were created via the sol-gel procedure in the absence and presence of Polyvinylpyrrolidone (PVP) as an organic modifier. bioglass/maltdextrin nanoparticles and bioglass/maltdextrin/PVP nanocomposites were characterized by (XRD) technique, (EDX), (FE-SEM) and (FT-IR). Moreover, the loading of flutamide and release behavior at pH = 7.4 and T = 37 °C of the provided specimens were determined by UV-Vis Spectroscopy. The effects of flutamide Loading on the bioglass/maltdextrin/PVP nanocomposites at different times (6, 8, 24 and 72 hrs.) were investigated. Also, the structural properties of bioglass / maltodextrin / PVP nanocomposites on loading and release of flutamide were evaluated. The capability of nanocomposites for flutamide delivery was surveyed as a drug delivery pattern under in vitro condition. Percentage of Drug loading efficiency on nanocarriers 99.89% was acquired, and eventually the release rate was reduced slowly up to nearly 12 days. Accordingly, the outcomes ascertained that the bioglass/maltdextrin/PVP nanocomposites with the high loading performance and stable release ability can be appropriate candidates for sustained flutamide release.

**Keywords:** *Efficiency; Nanoparticles; Prostate Cancer; Release; Sol-gel.*

**How to cite this article**

*Tajik M., Seyed Sadjadi M., Zare K., Farhadyar N. Synthesis and characterization of bioglass / maltodextrin nanocomposites in the presence of PVP as a potential candidate for flutamide drug delivery. Int. J. Nano Dimens., 2022; 13(4): 362-373.*

## INTRODUCTION

Human body damages, particularly in hard tissues such as bone, hip, knees, teeth and hamstring cause significant hardness to human kind [1]. Bio glass nanoparticles are one of the majorities widely developed nanotechnology materials because of their bioactive properties and mechanical efficiency, which can be widely used in bone tissue engineering, bone graft materials for bioactive coating for orthopedic implants, and as filler particles in polymer composites [2]. The increasing need for artificial substitution parts which can be used to repair and to reconstruct disease or defective part is warning. Nowadays, the need of framework to grow and engineer soft tissues has also increased, the recent scaffolds are been graded as regenerative medicines. Also, the recent tendency involves the progress of nanostructured materials to enhance their biocompatibility [3]. The most importantly used bioactive materials for bone regeneration are hydroxyapatite and tricalcium phosphate as well as bioactive glasses. And so, hydroxyapatite (HA,

* Corresponding Author Email: *m.s.sadjad@gmail.com*

**This work is licensed under the Creative Commons Attribution 4.0 International License.**
To view a copy of this license, visit http://creativecommons.org/licenses/by/4.0/.

$Ca_{10}(PO_4)_6(OH)_2$) (HAP) is a naturally occurring mineral and the most important component of vertebrate bone and tooth enamel. However due to the fragile nature of porous HAP, it can be applied only in non-loading sites [4]. In general, synthetic hydroxyapatite is widely applied in dental, craniofacial and orthopedic surgery, majority as granules and as bioactive coating on load bearing implants. HAP is osteoconductive, biocompatible and practically inert; it is resolved with time, but releases at a slower rate [5]. Bioactive glasses were made of $SiO_2$-CaO-$P_2O_5$-$Na_2O$ system, which have been displayed to form a mechanically strong bone and soft tissue bonding does happens the fast formation of a thin layer of hydroxycarbonate apatite or hydroxyapatite (similar to biological apatite) on the glass surface when implanted or in contact with biological fluids [6-8]. The glass will be absorbed and eventually displaced bone because all of the components in the bio glass are physiological chemicals found in the body (silicone, sodium, potassium, magnesium, oxygen, calcium, phosphorus). It has also been displayed those bioactive glasses produce an ideal environment for colonization, proliferation and differentiation of human Osteoblasts to form a new bone. Since bioactive glasses are able to form bonds to soft tissues, the concatenation of bioactive glass particles either as coatings or fillers into composing ceramic/polymer framework is seen as a comfortable way to create structure for tissue engineering applications [9-11]. Bio glass nanoparticles are very significant in the biomedical field due to their unique characteristics, namely osteoconductive and osteoinductivity, and under certain conditions, they are also angiogenic and bactericidal [12]. Bio glass can react with physiological fluids to form intense bonds with the bone. The bonding will be followed by the release of ions in the formation of the hydroxycarbonatepatite (HCA) layer and the biological interaction of collagen with the glass surface so that these various reactions are very beneficial in the care process of bone fractures [13]. The composition of bio glass nanoparticles with a polymer system is capable of producing a nanocomposite that has the potential for usage in orthopedic applications, containing tissue engineering and tissue regeneration. The composite improvement that is biodegradable with polymers also allows the production of a substrate that can trigger the bio mineralization process [14]. Various methods such as the sol-gel [15], flame method [16], microwave irradiation synthesis [17], and micro emulsion [18] were accomplished to synthesize bio glass nanocomposites, two main operations that can synthesize this biomaterial are the melt quenching procedure and sol-gel method. The melt quenching procedure can synthesize bio glass in a concise time, about several hours, by heating the initial precursors to increase temperatures and following particular principles. Although the melt technique is an immediate procedure, the outcoming glass usually has a low particular surface area value. Subsequent to the previous investigation, the specific surface area value is a key agent affecting bio glass bioactivity [19-20]. Increasing the specific surface area can increase the surface reaction between the dummy material and the physiological environment, then incrementing the formation of the HA layer. The sol-gel method can synthesize bio glass at lower temperatures, has a porous structure, and a high special surface area value that can increment the bioactivity of synthetic materials [21]. Ramteke et al. evaluated the optimized crystal growth of potassium aluminium sulfate (KAS) at diverse pH. The well-defined single KAS crystals have been grown at pH 3, 5 and 7 involving the slow vaporization process. The impact of pH on optical lucidity of KAS crystal is investigated within 200–1000 nm through UV–visible optical analysis. He-Ne laser assisted Z-scan procedure is applied to analyze third order nonlinear optical (TONLO) virtues of KAS crystal grown at similar pH [22]. Anis et al. investigated Up-gradation of novel period photonic apparatus encourages modelling of nonlinear optical crystal that encompass excellent linear–nonlinear optical properties. This is the first attempt to modify the optical performance of zinc tris-thiourea sulphate (ZTS) crystal using L-tyrosine (Ty). The energy-dispersive spectroscopy is employed to demonstrate the insertion of Ty. Single-crystal XRD analysis is used to distinguish the structural parameters. The 5% increase in transmittance of ZTS crystal due to Ty has been measured by UV–visible study. Kurtz–Perry experiment authenticated that frequency doubling capability of Ty-ZTS crystal is 1.71 times higher than ZTS. The incidence of photoluminescence nature has been studied within visible region [23]. Baig *et al.* studied the doping of amino acid $_L$-valine (LV) to modify the optical and dielectric functions of bis-


CC BY

thiourea cadmium chloride (BTCC) crystal to investigate it monopolize efficiency for nonlinear optical devices. The structural constants of pristine and LV-doped BTCC crystal were acquired through monocrystal XRD analysis [24]. The synthesis of bioactive glass nanocomposites in the presence and absence of PVP is one of the most favorable and efficient methods for creating the bio glass bioactivity for various applications. Therefore, in the present research, a novel and simple method are applied to fabricate bioactive glass nanocomposites based on maltodextrin in the presence of PVP. To the best of our knowledge, there is no study on the synthesis of bioactive glass nanocomposites with controlled size in the presence of PVP. On the report of the findings from the prevalent study, the chemical, crystalline and morphological properties of prepared nanoparticles are importantly affected by presence of PVP. Bioglass/maltodextrins/ PVP nanocomposites prepared in this paper answer almost all appearance for a proper carrier such as biocompatibility and biodegradability for high loading of flutamide drug due to suitable structure bioglass/maltodextrins. As the outcomes display, the suitable structure of nanocomposites synthesized in this study is significantly effective in drug delivery compared with the previous studies [11-12]. Our purpose in this study to find a crystal and a pore size controllability method for synthesis and characterization of bioactive glass nanocomposites based on maltodextrin and so, flutamide Loading on the bioactive glass nanocomposite at different times (6, 8, 24 and 72 hrs.), at pH = 7.4 and T = 37 °C were investigated. Also, the structural characteristics of the bioactive glass / maltodextrin nanoparticles in the flutamide Drug loading and release were studied. Our research demonstrated that Due to the flutamide non-steroidal structure, it has fewer hormonal side effects than other drugs but owing to the rare side effects of acute hepatotoxicity, it should be taken in long-term and lower doses. And bioglass/ maltodextrins/ PVP nanocomposites with constant and slow-release ability can be a good election for this purpose.

## EXPERIMENTAL

*Material*

All chemicals, Polyvinylpyrrolidone (PVP), Maltodextrin, $Ca(NO_3)_2.4H_2O$, $(C2H5O)_4Si$, $NH_4H_2PO_4$, $NaNO_3$, $Ca(NO_3)_2 \cdot 4 H_2O$, phosphate buffer solution (PBS), sulfuric acid (98%), nitric acid (70%), and HCl solutions (5%) were acquired from Merck company. The active component of the drug flutamide was prepared from Sobhan Pharmaceutical Chemistry Company, in Iran. Analytical grad chemicals were applied for all investigations with no extra material. Distilled water was used for all evaluated investigations.

*Synthesise of bioactive glass nanoparticles based on maltodextrin in the absence of pvp*

The bio glass was prepared by the sol-gel method; the precursor used in this study was Tetraethyl orthosilicate (TEOS). Dissolve 2 g of maltodextrin in ionized water and stir for 1 hour at 80 °C, setting the pH to 2 and stirring. Add 20 mL of ortho-tetra ethyl silicate and stirring in the room for 1 hour. Add 8.75 g of calcium nitrate hydrate and the solution was stirred to dissolve 6.75 g of sodium nitrate, the following add 1.2 g of ammonium dihydrogen phosphate and the solution was stirred for about 1 hrs to obtain homogenous gel. Then the material was ultrasonic for 1 hour, and then for 3 hrs in the oven at 100 °C to prepare a sample.

*Synthesis of nanocomposites based on bioactive glass/ maltodextrin in the presence of PVP*

2 g of maltodextrin dissolve in a 2% solution of Polyvinylpyrrolidone (PVP) and distilled water. Then, the solution was stirring for 1 hrs at 80 °C and the pH level was maintained above 10 under stirring for 15 min. 20 mL of tetraethyl silicate was added and stirred in the room for 1 hr. Then, 8.75 g of calcium nitrate hydrate was added slowly to the mixture during the stirring process to dissolve. So, 6.75 g of sodium nitrate was added, and then, 1.2 g of ammonium dihydrogen phosphate was added and stirring for about 1 hour to form a jelly-like structure. Then, the material was place in the ultrasonic for 1 hour, and dried in a vacuum oven at 100 °C for 3 h until the desired sample is prepared (Fig. 1).

*Loading step of flutamide on the bioglass/ maltdextrin nanocomposite in the presence of PVP*

1 mg of the synthesized nanocomposite is stirred in the presence of 10 mL of flutamide solution with an intensity of 10-100 PPM at different times of hours 6/8/24/72 hours. The calibration curve line equation is used to determine the amount of drug loaded on the


(cc) BY

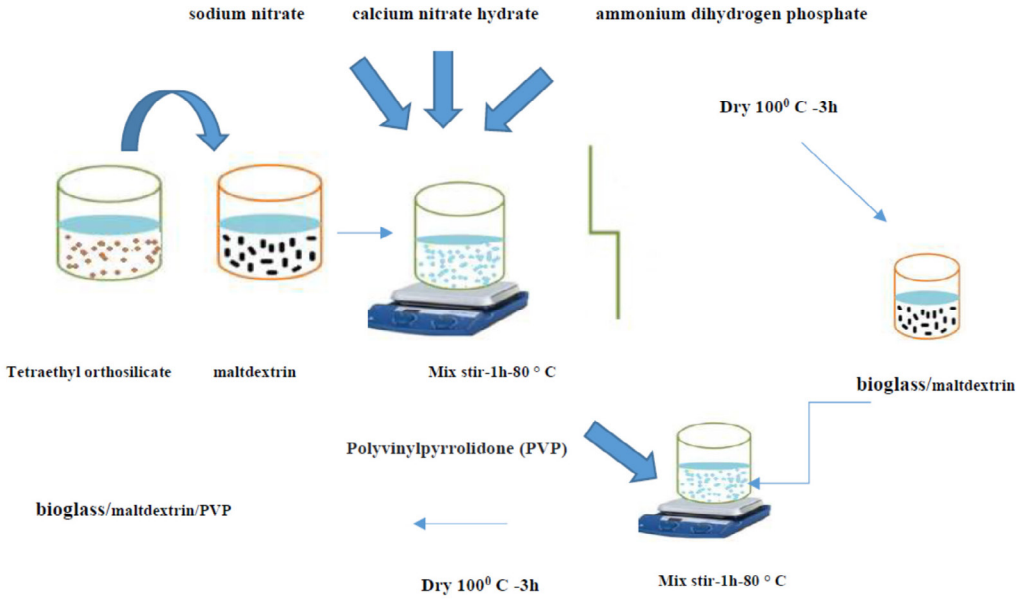


Fig. 1. The preparation procedure of bioglass/maltdextrin/PVP nanocomposite.

bioglass/maltdextrin nanocomposite. Drug loading with the loaded drug is calculated according to the total loaded drug as well as the amount of nanocomposite and confinement efficiency. As a result, drug content, drug loading, encapsulation efficiency was Determined.

*Characteristics of flutamide loading in extracorporeal environment in the simulated intestinal environment*

3 mg of the dried nanostructure is poured into 5 mL of phosphate buffer at pH = 7.4 in a 100 beaker and placed in a shaker under stirring at 90 rpm. At regular intervals for 8 hours (approximately every 50 minutes) each time 1 mL was removed from the solution using a sampler and centrifuged for 15 minutes, the upper solution was separated to read the adsorption and the lower solution was returned to the beaker containing the initial solution. To keep constant the volume of release environment each time a sample is taken with a sampler, 1 mL of the buffer replacement of the solution is removed. These steps were performed in 8 steps. The adsorption of these 8 solutions at the maximum wavelength (nm) of standard drug solutions was called. During the drug test in the buffer solution, the beaker contains samples is placed on a stirrer at regular intervals for 48 hours (approximately every 4 hours). The upper solution was separated to read the adsorption and the lower solution was returned to the beaker containing the initial solution. To keep constant the volume of release environment each time a sample is taken with a sampler, 1 mL of the buffer replacement of the solution is removed. These steps were performed in 12 steps. Each time 1 mL of the solution was removed using a sampler and centrifuged for 15 minutes, the upper solution was separated to read the adsorption and the lower solution was returned to the beaker containing the initial solution. The adsorption of these 12 solutions at the maximum wavelength (227 nm) was called standard drug solutions.

The Percentage of drug release in buffer solution was obtained from the following equation:

Mt / Mn * 100

Mt of drug released at each step and Mn more concentration of drug released.

## RESULTS AND DISCUSSION

*X-ray Diffraction Analysis*

XRD patterns of the samples were recorded in ambient air by using a Philips Xpert XRD. Fig. 2(a, b) illustrates the XRD patterns of bioglass/ maltdextrin nanocomposite in the absence and presence of Polyvinylpyrrolidone (PVP). The average crystallite size for bioglass/maltdextrin nanocomposite doped with 2% concentration of PVP from the range of 10-60nm was deliberated by using standard Debye-Scherrer equation $D$ =


(cc) BY

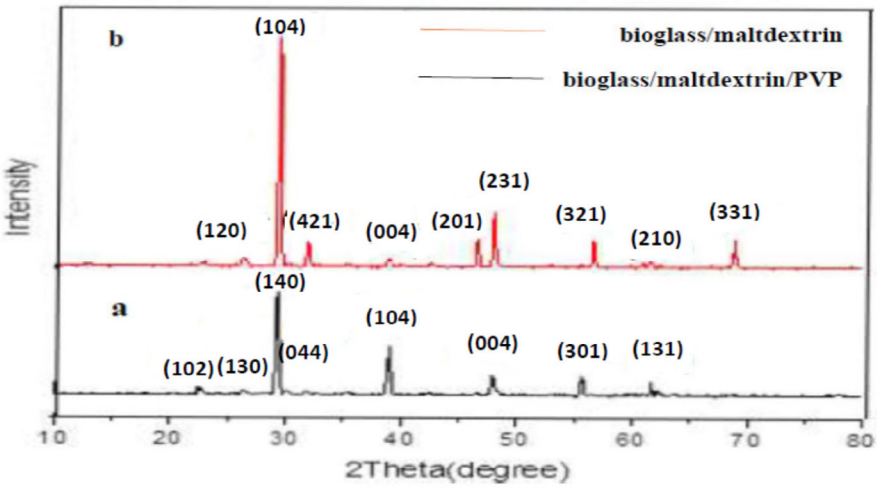


Fig. 2. XRD patterns of the, a**)** bioglass/maltdextrin/PVP nanocomposite, b) bioglass/maltdextrin**.**

Table 1. Structural parameters acquired from XRD patterns analysis.

| Sample | Cell parameters (Å) | Volume(Å)$^3$ | Structure |
|---|---|---|---|
| bioglass/maltdextrin | a=10.03 b=9.80 c=7.03 | 679.22 | Monoclinic |
| bioglass/maltdextrin/PVP | a=12.94 b=8.63 c=5.39 | 602.47 | Monoclinic |

0.9λ/(βcosθ) [25], where D indicates the diameter of the nanoparticles, λ (Cu Kα) =1.5406 A° and *β* represents the full-width at half maximum of the diffraction lines. Our results acquired from calculation of D values are displayed in Table 1. Accordingly, cell constants calculated were using Eq. (1).

$$\frac{1}{d^2} = \frac{4}{3}\left(\frac{h^2+hk+k^2}{a^2}\right) + \frac{l^2}{c^2} \quad (1)$$

(h, k, l) demonstrate miller indices, d represents interplanar spacing, and (a, c) define lattice constants. The computed cell constants are presented in Table 1. The characteristic diffraction peaks were observed at 22.60°,27.44°, 30.14°, 36.89°,38.67°, 49.45°,55.04° and 64.22°corresponding to the (102), (130), (140), (044), (104), (004), (301) and (131) planes of bioglass/maltdextrin/PVP nanocomposite (Fig. 2). As can be observed, that the sharpest peak related to 2θ = 30.14°. As can be observed in Figs. 2a and 2b respectively, at pH=7.4 bioglass/ maltdextrin nanocomposite in presence and absence of Polyvinylpyrrolidone (PVP) is alike to the XRD patterns, and diffraction peaks can be attributed to the monophasic low crystalline Polyvinylpyrrolidone (PVP). Broadening of the peaks in XRD pattern of bioglass/maltdextrin nanocomposite following incrementing the concentration PVP at pH=7.4 can be indicate of formation of nanostructured materials, reduced size of the bioglass/maltdextrin/ PVP nanocomposite, and crystallinity in the presence of matrix of biopolymers [26, 27]. The conclusions determined that the crystallite size and cell constants decreased with doping of Polyvinylpyrrolidone (PVP). Concentration can be illustrated by the effect of PVP doping on the crystalline size.

*Fourier Transform Infrared Spectroscopy (FT-IR)*

Fig. 3 shows FT-IR spectra of bioglass/ maltdextrin/PVP nanocomposite at pH value of 7. In the spectrum of bioglass/maltdextrin/ PVP, bands at 3447, 3383, 3131, 2924, 2448 and 1716 were assigned to O–H stretching, $CH_2$ stretching vibration of asymmetric pyrrole ring groups, $CH_2$ stretching vibration of symmetric pyrrole ring groups and O=C vibration of carbonyl group respectively. The bending vibration of (C-H), $CH_2$ and (N-C=O) groups appeared at around 1262 $cm^{-1}$, 1134 $cm^{-1}$ and 1068 $cm^{-1}$ respectively. Another peak appeared at the 954$cm^{-1}$, which


CC BY

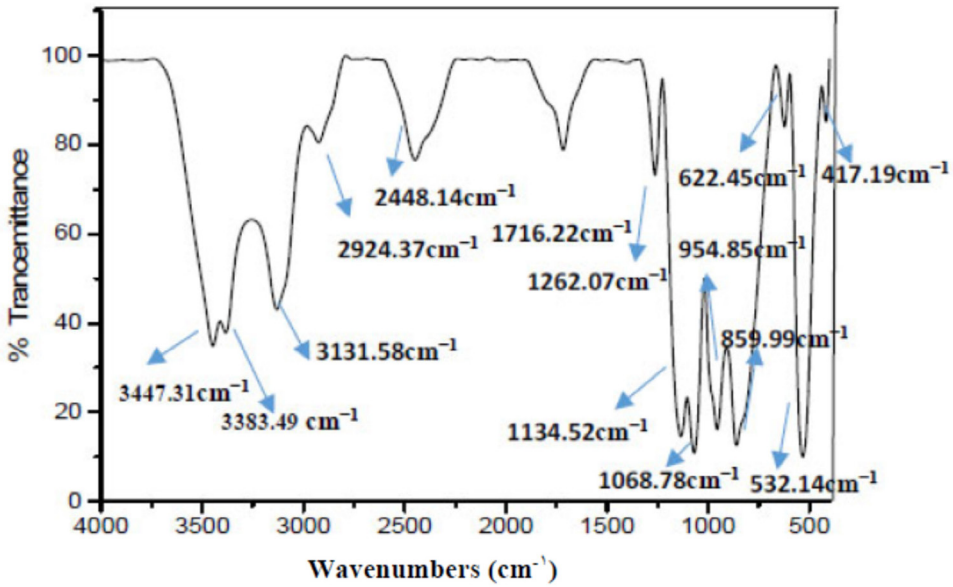


Fig. 3. FT-IR spectra of the bioglass/maltdextrin/PVP nanocomposite.

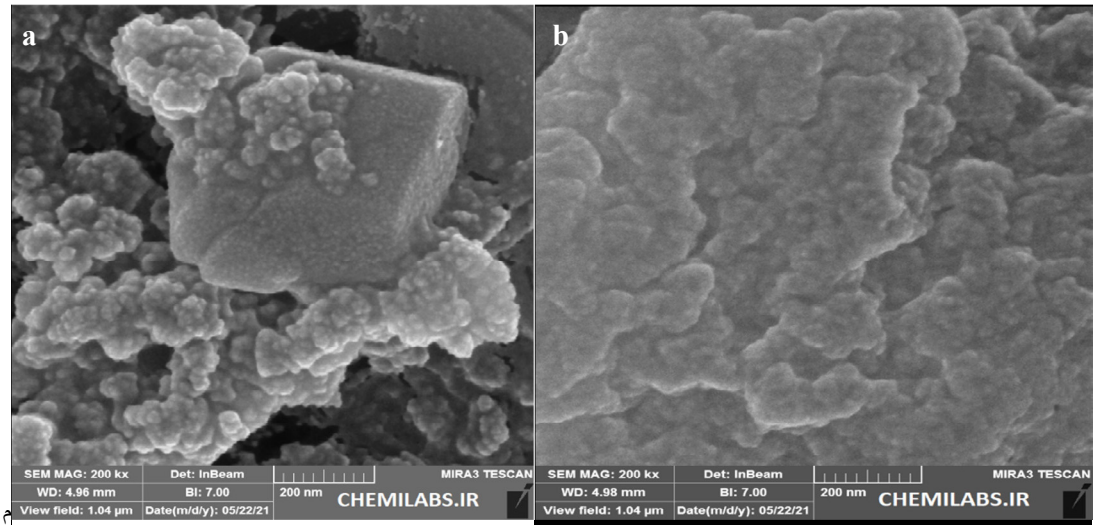


Fig. 4. FE-SEM images of a**)** bioglass/maltdextrin, b**)** bioglass/maltdextrin/PVP.

could be attributed to the C-$H_2$ wagging ν(C-N) stretching. The band at 859 $cm^{-1}$ and 622 $cm^{-1}$ is attributing to the stretching vibration of C-C, $CH_2$ rock and C-C bond [28]. In addition, the spectra of bioglass/maltdextrin/PVP nanocomposites which could certified the presence of PVP based on the absorption bands of bioglass/maltdextrin nanocomposite about 532 $cm^{-1}$ and 417 $cm^{-1}$. There were slight shifts in the position of absorption bands for the Polyvinylpyrrolidone (PVP) prepared in the presence of bioglass/maltdextrin demonstrating dissociation and interaction of bioglass/maltdextrin with nucleating crystals [29].

*Morphology and element analysis*

The morphology of the specimens was analyzed utilizing FESEM (Fig. 3a, 3b) and EDX (Fig. 5a, 5b). FE-SEM was applied to obtain morphological characteristics of the samples. Fig. 4 displays the images of synthesized nano bioglass/maltdextrin nanocomposites in the absence (a)


(cc) BY

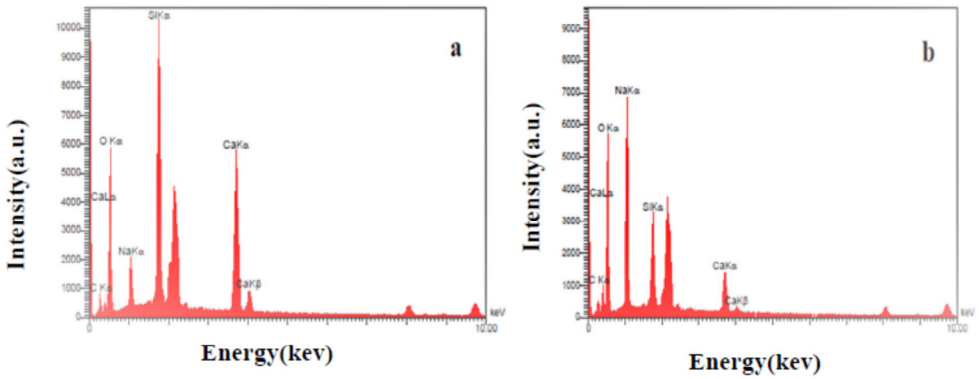


Fig. 5. EDS images of a) bioglass/maltdextrin, b) bioglass/maltdextrin/PVP.

Table 2. EDX quantifcation elements of bioglass/maltdextrin and bioglass/maltdextrin/PVP.nanocomposite.

| Elementray At % calculated from EDX analysis | | |
|---|---|---|
| Element | bioglass/maltdextrin | bioglass/maltdextrin, /PVP |
| C | 11.11 | 10.42 |
| O | 51.98 | 45.93 |
| Na | 8.10 | 29.30 |
| Si | 19.89 | 11.26 |
| Ca | 8.93 | 3.08 |

and presence (b) of Polyvinylpyrrolidone (PVP) at pH values of 7. It sees Polyvinylpyrrolidone (PVP) that all over morphology of the nanocomposites created in the presence and absence of Polyvinylpyrrolidone (PVP) polymer is spherical. Micrographs indicated that presence the Polyvinylpyrrolidone (PVP) in nano bioglass/ maltdextrin composites can be the cause of distribution of spherical particles by smaller crystallite sizes due to interaction between $OH^-$ and the carbonyl group of biopolymers on surface of nano bioglass/maltdextrin composites. For synthesized samples, the amounts of elements of the surfaces were assessment via EDX analysis. Fig. 5a shows the presence of carbon (C), sodium (Na), oxygen (O), silicon (Si) and calcium (Ca) in bioglass/maltdextr nanocomposites, for the bioglass/maltdextrin/PVP nanocomposites (Fig. 5b). According to the Table. 2, Elementray At % in nanocomposites have been reduced which indicates the presence of PVP in bioglass/ maltdextrin/PVP nanocomposite structure.

*Investigation of calibration curve in phosphate buffer solution*

The amount of 0.0015 g (1.5 mg) of the drug was solved in 2.5 mL of methanol, and in the 50-cc beaker with phosphate buffer pH = 7.4. 30 ppm initial solution was obtained. From this solution, the concentrations of 1, 3, 5, 7, 10, 15 ppm were volume in the 50 mL buffer with phosphate buffer. Initial solution was determined in ultraviolet spectroscopy during 282 nm wavelength. Concentrations of 1 to 15 ppm were checked out in this absorption wavelength and according to the Fig. 6 the calibration diagram of the drug was drawn in the phosphate buffer solution. Using the calibration curve of secondary drug solutions and the rate of free drug absorption in a nanoparticle solution, according to the table 2, the concentration of free drug in the solution was calculated in ppm. According to the line equation (2), the concentration of nanoparticles loaded with drug was obtained and also, the measurement of the drug loading was deliberated according to the


CC BY

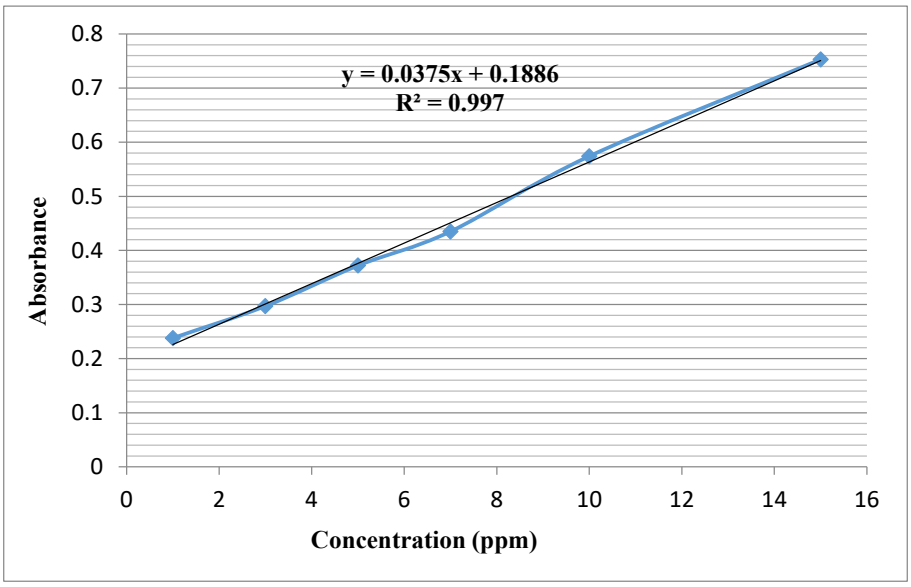


Fig. 6. Drug calibration diagram in phosphate buffer solution.

**Table 3.** Adsorption of dilute drug solutions in phosphate buffer solution (ppm).

| Conc (ppm) | Abs. |
|---|---|
| 1 | 0.238 |
| 3 | 0.297 |
| 5 | 0.372 |
| 7 | 0.435 |
| 10 | 0.574 |
| 15 | 0.753 |

weight percentage of the loaded drug to on the total value of the loaded drug and as well as this values the nanocomposites Eq. (2).

y = 0.0375x + 0.1886 (2)
=0.213 0.0375x + 0.1886
x=0.6506 mg/l (ppm) = 0.00065 mg/ml

(1.5 mg) of the drug was solved in 2.5 mL methanol:
(Initial drug amount): 1.5 mg
(The volume of methanol solvent for drug solving): 2.5 mL
(Initial drug concentration):1.5 / 2.5 = 0.6 mg/ml

Loading the drug efficiency (%): x-y/x *100 (3)
The amount of initial drug concentration= x and y = the amount of wasted drug concentration
Drug loading efficiency on nanocarriers (%): = 0.6 - 0.00065 /0.6 *100 = 99.89%

*flutamide release in phosphate buffer solution*

According to the line equation obtained from the calibration curve Eq. (4), the status of each step is obtained. (Instead of absorbing the released drug, it is placed in a phosphate buffer solution and the drug is released). The release concentrations of the drug in phosphate buffer solution are given in Table 3.

y = 0.0375x + 0.1886 9 (4)

The amount of drug released in the phosphate buffer solution= **X/1000** mg/ mL
We obtained drug release from the following relation:

drug release (%)= Mt/Mn*100
Mt: of drug released at each steps Mn: more concentration of drug released.


(cc) BY

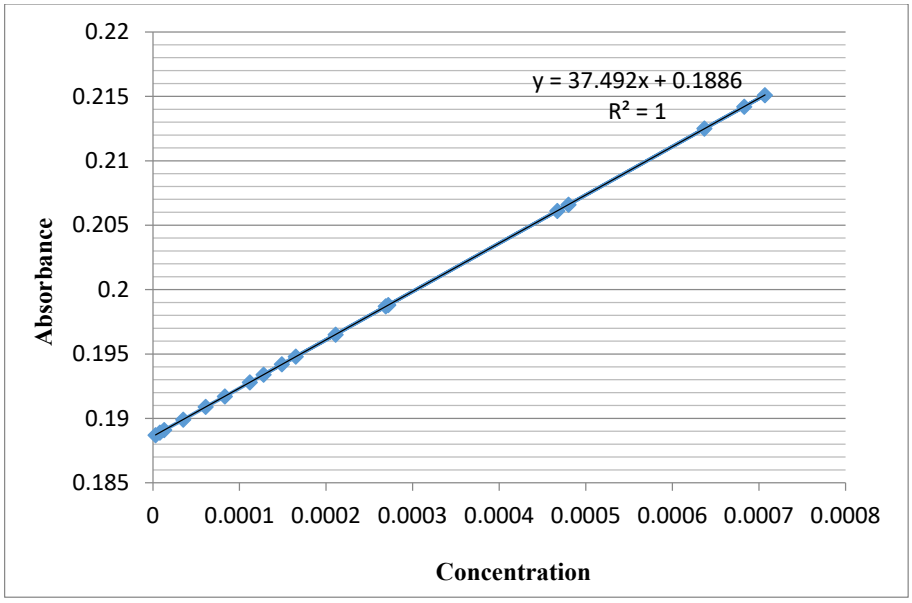


Fig. 7. Adsorption of drug released in buffer solution by increasing drug concentration in phosphate buffer solution.

**Table 4.** Release of drug in phosphate buffer solution.

| Time(hours) | absorbance | The concentration of released drug in (mg \ml) | The concentration of released drug in (mg \ml) | %Drug release |
|---|---|---|---|---|
| 1 | 0.1887 | 0.003 | 0.000003 | 0.42 |
| 2 | 0.1889 | 0.008 | 0.000008 | 1.13 |
| 3 | 0.1891 | 0.013 | 0.000013 | 1.84 |
| 4 | 0.1899 | 0.035 | 0.000035 | 4.95 |
| 5 | 0.1909 | 0.061 | 0.000061 | 8.63 |
| 6 | 0.1917 | 0.083 | 0.000083 | 11.74 |
| 7 | 0.1928 | 0.112 | 0.000112 | 15.84 |
| 8 | 0.1942 | 0.149 | 0.000149 | 21.07 |
| 12 | 0.1965 | 0.211 | 0.000211 | 29.84 |
| 16 | 0.1988 | 0.272 | 0.000272 | 38.47 |
| 20 | 0.2066 | 0.48 | 0.00048 | 67.89 |
| 24 | 0.2151 | 0.707 | 0.000707 | 100 |
| 28 | 0.2142 | 0.683 | 0.000683 | 96.61 |
| 32 | 0.2125 | 0.637 | 0.000637 | 90.10 |
| 36 | 0.2061 | 0.467 | 0.000467 | 66.05 |

*Investigation of flutamide loading in vitro stable release*

The nanocomposites bioglass/maltdextrin/PVP has many profits in drug mechanisms of action. Polar groups such as the OH, N = O, or $CH_2OH$ can to be mixed with flutamide molecules via van der walls forces and hydrogen bonding, which can be desirable for the drug loading. For illustrating these advantages, in this research, the capability of elected carriers to catch flutamide using the specifications of a carrier (Drug loading efficiency) was investigated. In Fig. 7 and Table 4, we have briefed the drug loading efficiency of the synthesized specimens. The sustained release of flutamide in the samples happened through the slow dissolution procedures. Fig. 8 shows the release of flutamide from the bioglass/maltdextrin/PVP nanocomposites at 35 °C and pH 7.4. The initial release of flutamide happened within the first 24 h. After that, the rate of release substantially reduced up to around 12 day, as the drug released gradually from the layers in

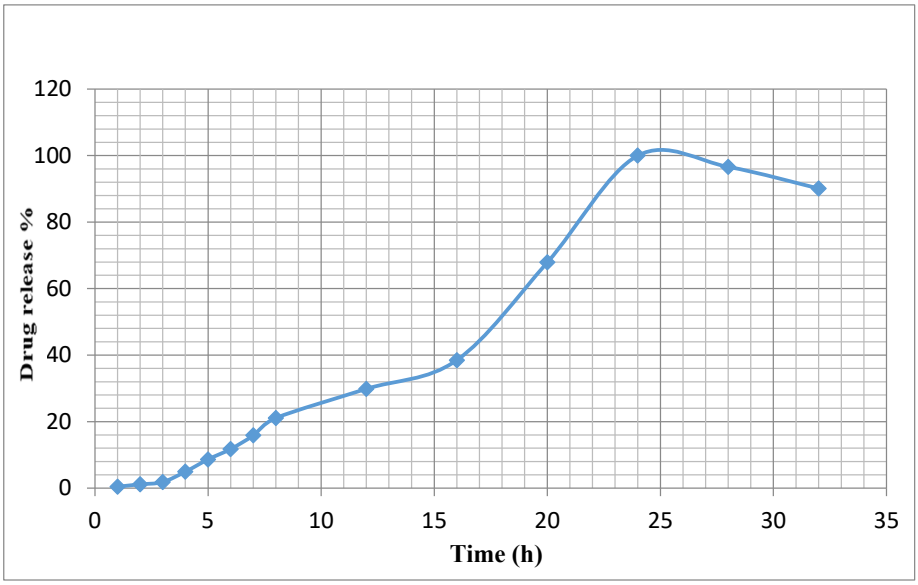


Fig. 8. Percentage of drug release in phosphate buffer solution per unit time (hours).

the bioglass/maltdextrin and PVP carriers. The results demonstrated that the flutamide loaded on nanocomposites has a long release time and permanent release capacity. The release of flutamide from bioglass/maltdextrin/PVP nanocomposites has been 99.89 %, after 12 days, (refer to Fig. 8), which can be consequence from drug molecules imbedded in nanocomposites. The flutamide drug included in the nanocomposites could release to the surrounding Prostate cancer cells and the cancer cells region would be diminished. As displayed in Table 4, in evaluation to previous researches, the nanocomposites synthesized in this research with their flutamide high loading performance as well as sustained release capacity can as to be proper candidates for flutamide drug delivery.

## CONCLUSION

In the present study, bioglass/maltodextrins nanocomposites were prepared successfully by sol-gel approach in the absence and presence of PVP for flutamide drug delivery. According to the results from the current study, the chemical, crystalline and morphological properties of provided samples are outstandingly affected by Polyvinylpyrrolidone (PVP) content. FT-IR findings demonstrated that strong chemical interactions happen between organic and inorganic components and that the specimens are composed of two phase's bioglass/maltodextrins nanocomposites and Polyvinylpyrrolidone (PVP). Based on XRD analysis findings, it is showed that the place of the peaks with add Polyvinylpyrrolidone (PVP) shifted little to the higher angles, that can be owing to the incorporation of PVP in the bioglass/maltodextrins nanocomposites structure that cause be to the deviation of the angles. Morphological resulting in the bioglass/maltodextrins/ PVP nanocomposites affirms that Polyvinylpyrrolidone (PVP) and bioglass/maltodextrins nanoparticles have been successfully combined and have been prepared nanocomposites with size less70 nm. The ability of the nanocomposites to drug delivery flutamide in vitro at different times (6, 8, 24 and 72 hrs.), at pH = 7.4 and T = 37 °C was investigated. The findings divulged that the synthesized nanocomposites have a high capability to load flutamide. Flutamide release studies in PBS displayed, that initial release for all specimens happened within the first 24 h, and constantly the release rate was decreased moderately up to nearly 12 days, as the drug released gradually from the layers in the bioglass/ maltodextrins and Polyvinylpyrrolidone (PVP) nanocomposites. Flutamide -loaded specimens demonstrated a slow, long-term, and constant release rate in PBS. The above- cited profits can detract the pain for patients and construct a more suitable condition for prostate cancer. However, it was arduous to evaluate the consequences of this


(cc) BY

research with prior investigations owing to the application of unlike conditions, but, as can in Table 3 be observed, the present work was found that synthesized specimens in this investigation can be good candidates for flutamide drug delivery. Also, because of its non-steroidal structure, flutamide has fewer hormonal side effects than other drugs and does not affect kidney function, but due to the rare side effects of acute hepatotoxicity, it should be taken in longer and lower doses. And bioglass/maltodextrins/ PVP nanocomposites with permanent and slow-release capability can be a good choice for this purpose. It is hoped that in the near future, due to the high ability of bioglass/ maltodextrins/ PVP nanocomposites to load flutamide, it will be evaluated in the loading of other drugs and will be effective and useful in the treatment and prevention of other cancers with the ability of permanent release and durability.

**ACKNOWLEDGEMENT**

We thank science and research Branch, Islamic Azad University Tehran for supporting this research and Iran Nanotechnology Initiative.

**CONFLICTS OF INTEREST**

The authors do not have any conflicts of interest.

**REFERENCES**

[1] Durgalakshmi D., Subhathirai S. P., Balakumar S., (2014), Nano-bioglass: A versatile antidote for bone tissue engineering problems. *Procedia Eng.* 92: 2-8.

[2] Widiyanti S., (2020), Synthesis of nano bioactive glass or bioglass. *Green Appl. Chem.* 10: 01-32.

[3] Chai C., Leong K. W., )2007(, Biomaterials approach to expand and direct differentiation of stem cells. *Molec. Therap.* 15: 467-480

[4] Dinarvand P., Seyedjafari E., Shafiee A., Babaei Jandaghi A., Doostmohammadi A., Fathi M. H., Soleimani M., (2011), New approach to bone tissue engineering: Simultaneous application of hydroxyapatite and bioactive glass coated on a poly (L-lactic acid) scaffold. *ACS Appl. Mater. Interf.* 3: 4518-4524.

[5] Miao X., Tan D. M., Li J., Xiao Y., Crawford R., (2008), Mechanical and biological properties of hydroxyapatite/ tricalcium phosphate scaffolds coated with poly (lactic-co-glycolic acid). *Acta Biomater.* 4: 638-645.

[6] Kuzmenka D., Sewohl C., König A., Flath T., Hahnel S., Schulze F. P., Schulz-Siegmund M., (2020), Sustained calcium (II)-release to impart bioactivity in hybrid glass scaffolds for bone tissue engineering. *Pharmaceutics*. 12: 1192-1197.

[7] Huang L. D., Gong W. Y., Dong Y. M., (2021), Effects of bioactive glass on proliferation, differentiation and angiogenesis of human umbilical vein endothelial cells. *J. Peking Univ. Health Sci.* 53: 371-377.

[8] Sedighi O., Alaghmandfard A., Montazerian M., Baino F., (2022), A critical review of bioceramics for magnetic hyperthermia. *J. Am. Ceram. Soc.* 105: 1723-1747.

[9] Gerasymchuk Y., Wedzynska A., Lukowiak A., (2022), Novel $CaO–SiO_2–P_2O_5$ nanobioglass activated with hafnium phthalocyanine. *Nanomater.* 12: 1719-1725.

[10] Pajares Chamorro N., Wagley Y., Hammer N., Hankenson K., Chatzistavrou X., (2022), Bioactive glass particles as multi functional therapeutic carriers against antibiotic resistant bacteria. *J. Am. Ceram. Soc.* 105: 1778-1789.

[11] Correia B. L., Gomes A. T., Noites R., Ferreira J. M., Duarte A. S., (2022), New and efficient bioactive glass compositions for controlling endodontic pathogens. *Nanomater.* 12: 1577-1582.

[12] Vale A. C., Pereira P. R., Barbosa A. M., Torrado E., Alves N. M., (2019), Optimization of silver-containing bioglass nanoparticles envisaging biomedical applications. *Mater. Sci. Eng: C*. 94: 161-168.

[13] Chen Q., Roether J. A., Boccaccini A. R., (2008), Tissue engineering scaffolds from bioactive glass and composite materials. *Topics In Tissue Eng.* 4: 1-27.

[14] Boccaccini A. R., Erol M., Stark W. J., Mohn D., Hong Z., Mano J. F., (2010), Polymer/bioactive glass nanocomposites for biomedical applications: A review. *Compos. Sci. Technol.* 70: 1764-1776.

[15] Sepulveda P., Jones J. R., Hench L. L., (2001), Characterization of melt-derived 45S5 and sol-gel–derived 58S bioactive glasses. *J. Biomed. Mater. Res: An Official J. Soc. Biomater.* 58: 734-740.

[16] Brunner T. J., Grass R. N., Stark W. J., (2006), Glass and bioglass nanopowders by flame synthesis. *Chem. Communic.* 13: 1384-1386.

[17] Sarkar S. K., Lee, B. T., (2011), Synthesis of bioactive glass by microwave energy irradiation and its in-vitro biocompatibility. *Bioceram. Develop. Applicat.* 1: 3-8.

[18] Leite Á. J., Mano J. F., (2017), Biomedical applications of natural-based polymers combined with bioactive glass nanoparticles. *J. Mater. Chem. B*. 5: 4555-4568.

[19] Sharma A., Jain C. P., (2010), Preparation and characterization of solid dispersions of carvedilol with PVP K30. *Res. Pharmac. Sci.* 5: 49-56.

[20] Saroj A. L., Singh R. K., Chandra S., (2013), Studies on polymer electrolyte poly (vinyl) pyrrolidone (PVP) complexed with ionic liquid: Effect of complexation on thermal stability, conductivity and relaxation behaviour. *Mater. Sci. Eng: B*. 178: 231-238.

[21] Bui X. V., Ngo T. M. T., (2020), Synthesis and characterization of a highly ordered mesoporous bio-glass. *VNU J. Sci: Nat. Sci. Technol.* 36: 57-63.

[22] Ramteke S. P., Muley G. G., Baig M. I., Ibrahim A., Manthrammel M. A., Muzammil K., Anis M., (2022), Optimizing growth, linear and 3rd order nonlinear optical traits of potassium aluminium sulfate (KAS) crystal by tuning pH for photonic device applications. *Inorg. Chem. Communic.* 140: 109484-109488.

[23] Anis M., Muley G. G., Baig M. I., Khan W. A., Ramteke S. P., Massoud E. E. S., (2022), Optimizing first-, second-and third-order optical traits of zinc tris-thiourea sulphate (ZTS) crystal by l-tyrosine for photonic device applications. *Ind. J. Phys.* 33: 1-4.

[24] Baig M. I., Hussaini S. S., Ali H. E., Anis M., (2022), Analyzing L-valine effect on structural, mechanical, optical and electrical traits of bis-thiourea cadmium chloride (BTCC) crystal. *J. Mater. Sci: Mater. Electron.* 33: 8218-8225.



CC BY

[25] Aslibeiki B., Kameli P., Salamati H., Eshraghi M., Tahmasebi T., (2013), Superspin glass state in $MnFe_2O_4$ nanoparticles. *J. Magnet. Magnet. Mater.* 322: 2929-2934.
[26] Meskinfam M., Sadjadi M. S., Jazdarreh H., (2011), Biomimetic preparation of nano hydroxyapatite in gelatin-starch matrix. *Eng. Technol*. 52: 395-398.
[27] Sahba R., Seyed Sadjadi M., Sajjadi A. A., Farhadyar N., Sadeghi B., (2018), Preparation and characterization of friendly colloidal Hydroxyapatite based on natural Milk's casein. *Int. J. Nano Dimens.* 9: 238-245.
[28] Rahma A., Munir M. M., Prasetyo A., Suendo V., Rachmawati H., (2016), Intermolecular interactions and the release pattern of electrospun curcumin-polyvinyl (pyrrolidone) fiber. *Biolog. Pharmac. Bullet.* 39: 163-173.
[29] Senthilkumar S. R., Sivakumar T., (2014), Green tea (Camellia sinensis) mediated synthesis of zinc oxide (ZnO) nanoparticles and studies on their antimicrobial activities. *Int. J. Pharm. Pharm. Sci*. 6: 461-465.


(cc) BY